Investigation of the Exchange-Correlation Potentials of Functionals Based on the Adiabatic Connection Interpolation

Eduardo Fabiano,[*,†,‡] Szymon Śmiga,[¶] Sara Giarrusso,[§] Timothy J. Daas,[§] Fabio Della Sala,[†,‡] Ireneusz Grabowski,[¶] and Paola Gori-Giorgi[§]

†Institute for Microelectronics and Microsystems (CNR-IMM), Via Monteroni, Campus Unisalento, 73100 Lecce, Italy

‡Center for Biomolecular Nanotechnologies @UNILE, Istituto Italiano di Tecnologia, Via Barsanti, I-73010 Arnesano, Italy

¶Institute of Physics, Faculty of Physics, Astronomy and Informatics, Nicolaus Copernicus University, Grudziadzka 5, 87-100 Torun, Poland

§Department of Theoretical Chemistry and Amsterdam Center for Multiscale Modeling, Faculty of Science, Vrije Universiteit, De Boelelaan 1083, 1081HV Amsterdam, The Netherlands

S Supporting Information

ABSTRACT: We have studied the correlation potentials produced by various adiabatic connection models (ACMs) for several atoms and molecules. The results have been compared to accurate reference potentials (coupled cluster and quantum Monte Carlo results) as well as to state-of-the-art ab initio DFT approaches. We have found that all the ACMs yield correlation potentials that exhibit a correct behavior, quite resembling scaled second-order Görling-Levy (GL2) potentials and including most of the physically meaningful features of the accurate reference data. The behavior and contribution of the strong-interaction limit potentials have also been investigated and discussed.
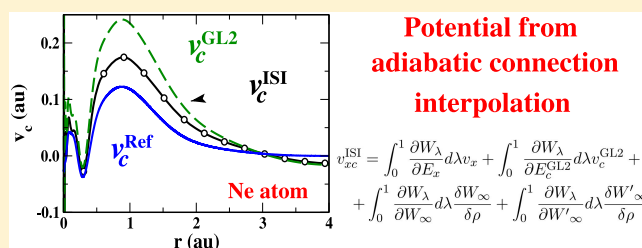
INTRODUCTION

The study of the exchange-correlation (XC) functional and the development of efficient and accurate approximations to it are among the main research topics in density functional theory (DFT). Within this theoretical framework, the XC functional describes in fact all the quantum effects of the electron−electron interaction, and it finally determines the accuracy of the overall computational procedure.

Over the years many different XC approximations have been developed,[1,2] and they are conventionally organized on the so-called Jacob's ladder of DFT.[3] To the highest rung of the ladder belong functionals that depend on the Kohn−Sham orbitals and eigenvalues. Some examples of these are the random-phase approximation,[4,5] double-hybrids functionals,[6,7] and the ab initio DFT methods.[8−10]

Another class of high-level XC approximations is the one of functionals based on interpolating the adiabatic connection integrand between its weak- and strong-interaction limits. These functionals use as a starting point the adiabatic connection formula[11−14]

$$E_{xc} = \int_0^1 W_\lambda[\rho] d\lambda \tag{1}$$

where ρ is the electron density, λ is the interaction strength, and $W_\lambda[\rho] = \langle \Psi_\lambda[\rho] | \hat{V}_{ee} | \Psi_\lambda[\rho] \rangle - U[\rho]$ is the density-fixed linear adiabatic connection integrand, with $\Psi_\lambda[\rho]$ being the wave function that minimizes $\hat{T} + \lambda \hat{V}_{ee}$ while yielding the

density ρ ($\hat{T}$ and $\hat{V}_{ee}$ are the kinetic and electron−electron interaction operators, respectively), and $U[\rho]$ being the Hartree energy. The task of constructing an XC approximation is then translated to the one of developing a proper approximation for the density-fixed linear adiabatic connection integrand W_λ[15] by interpolating between its known exact asymptotic behaviors in the weak- and strong-interaction limits,[16−19] i.e.

$$W_{\lambda \to 0}[\rho] \sim W_0[\rho] + \lambda W'_0[\rho] + \cdots \tag{2}$$

$$W_{\lambda \to \infty}[\rho] \sim W_\infty[\rho] + \frac{1}{\sqrt{\lambda}} W'_\infty[\rho] + \cdots \tag{3}$$

with

$$W_0[\rho] = E_x[\rho], \qquad W'_0[\rho] = 2E_c^{GL2}[\rho] \tag{4}$$

where E_x is the exact exchange, E_c^{GL2} is the second-order Görling-Levy (GL2)[16] correlation energy, $W_\infty[\rho]$ is the indirect part of the minimum expectation value of the electron−electron repulsion in a given density,[18] and $W'_\infty[\rho]$ is the potential energy of coupled zero-point oscillations.[19]

The functionals $W_\infty[\rho]$ and $W'_\infty[\rho]$ have a highly nonlocal density dependence, captured by the strictly correlated electrons (SCE) limit,[18−20] and their exact evaluation in

general cases is a nontrivial problem. Notice that while the form of the leading term $W_\infty[\rho]$ in eq 3 rests on recent mathematical proofs,[21,22] the zero-point term $W'_\infty[\rho]$ is a very reasonable conjecture that has been confirmed numerically in simple cases[23] but lacks a rigorous proof. The $\lambda \to \infty$ functionals can also be approximated by the much cheaper semilocal gradient expansions (GEA) derived within the point-charge-plus-continuum (PC) model[24]

$$W_\infty^{PC}[\rho] = \int \left[A\rho^{4/3}(\mathbf{r}) + B\frac{|\nabla\rho(\mathbf{r})|^2}{\rho^{4/3}(\mathbf{r})} \right] d\mathbf{r} \tag{5}$$

$$W'^{PC}_\infty[\rho] = \int \left[C\rho^{3/2}(\mathbf{r}) + D\frac{|\nabla\rho(\mathbf{r})|^2}{\rho^{7/6}(\mathbf{r})} \right] d\mathbf{r} \tag{6}$$

with $A = -9(4\pi/3)^{1/3}/10$, $B = 3[3/(4\pi)]^{1/3}/350$, $C = \sqrt{3\pi}/2$, and $D = -0.028957$. For small atoms, it has been shown that these PC approximations provide energies quite close to the exact SCE values.[18,19] More recently, new approximate functionals inspired by the SCE mathematical structure have been also proposed and tested.[25−27] They retain the nonlocality of SCE by using as a key ingredient some integrals of the density, and their implementation in a self-consistent scheme is still the object of ongoing work.

Different interpolation formulas have been employed to obtain several XC functionals based on the adiabatic connection formalism.[15,17,19,24,28−30] Some of these functionals have been recently tested against realistic physical chemistry problems in order to investigate their performance and understand the corresponding limitations.[31−33] These functionals are all size-extensive but not size-consistent when a system dissociates into fragments of different species. However, it has been recently shown that the size-consistency error can be easily corrected at no additional computational cost.[33] All these tests have concerned only the quality of the computed energies, whereas no information has been gathered on the XC potentials delivered by the functionals.

Actually, the XC potential is a very important quantity since it enters directly in the Kohn−Sham equations determining the quality of the Kohn−Sham orbitals and energies as well as the features of the electron density.[34−52] Thus, any accurate XC approximation should be able to yield not only precise energies at given densities but also accurate XC potentials. However, this fact is generally overlooked in most investigations of XC approximations, which mainly focus on the energy properties only. On the other hand, a few studies[36,38−43,53−59] have considered the problem of the XC potential showing that an accurate description of both the energy and the potential can be usually achieved only by high-rung approximations (although some important exceptions can be found at the meta-GGA level of theory[60,61]). The ability of an XC functional to describe correctly the XC potential is therefore a significant problem for DFT development.

In this paper, we consider some relevant XC functionals obtained by interpolating between the two limits of eqs 2 and 3, studying their ability to describe the XC potential. Obviously, this potential also depends on how the $\lambda \to \infty$ limit of eq 3 is approximated. We thus start by comparing the functional derivative of the PC model for the leading term, $W_\infty^{PC}[\rho]$ of eq 6, with the one from the exact SCE formalism for small atoms. Since the PC model is a GEA (and not a GGA), it diverges far from the nucleus. However, we find that in the

energetically important region, the PC functional derivative is a rather good approximation of the SCE potential, at least when evaluated on a given reference density (self-consistently the two will give very different results[20,62,63]). Moreover, because (due to the $\lambda \to 0$ expansion) all the considered approximations are complicated nonlinear functionals of the Kohn−Sham orbitals and eigenvalues, full self-consistent calculations have not been possible, regardless of how the $\lambda \to \infty$ limit is treated. Thus, as explained in the next section, the XC potentials have been computed for fixed reference densities and compared to accurate reference potentials as well as to the second-order Görling-Levy one. This approach was already successfully utilized in some studies[35,64] to investigate the XC potentials properties. Although the procedure does not provide access to the final self-consistent Kohn−Sham orbitals and density, it allows anyway to study the quality of the potential and the ability of each functional to reproduce its most relevant features. This work is therefore a fundamental first step toward the possible full self-consistent implementation of adiabatic-connection-based XC functionals.

◼ POTENTIALS FROM ADIABATIC CONNECTION MODELS

In this work we consider XC functionals based on different adiabatic connection models (ACMs) that use the input quantities of eqs 2 and 3, namely the exact exchange E_x, the second-order Görling-Levy correlation energy E_c^{GL2}, the strong-interaction limit of the density-fixed adiabatic connection integrand W_∞, and possibly the zero-point term W'_∞. In a compact notation, the XC functionals can be denoted as

$$E_{xc}^{ACM} = f^{ACM}(E_x, E_c^{GL2}, W_\infty, W'_\infty) \tag{7}$$

where f^{ACM} is an appropriate nonlinear function for the given ACM model. The exact expressions of the f^{ACM} functions corresponding to the functionals considered in this work, namely ISI,[15] revISI,[19] SPL,[17] and LB,[29] are given in Appendix A. Notice that ISI and revISI depend on all four input quantities, while SPL and LB do not depend on W'_∞. The XC potential corresponding to the functionals defined by eq 7 is

$$v_{xc}^{ACM}(\mathbf{r}) \equiv \frac{\delta E_{xc}^{ACM}}{\delta\rho(\mathbf{r})} =$$

$$= D_{E_x}^{ACM}\frac{\delta E_x}{\delta\rho(\mathbf{r})} + D_{E_c^{GL2}}^{ACM}\frac{\delta E_c^{GL2}}{\delta\rho(\mathbf{r})} + D_{W_\infty}^{ACM}\frac{\delta W_\infty}{\delta\rho(\mathbf{r})}$$

$$+ D_{W'_\infty}^{ACM}\frac{\delta W'_\infty}{\delta\rho(\mathbf{r})}$$

$$= D_{E_x}^{ACM}v_x(\mathbf{r}) + D_{E_c^{GL2}}^{ACM}v_c^{GL2}(\mathbf{r}) + D_{W_\infty}^{ACM}\frac{\delta W_\infty}{\delta\rho(\mathbf{r})}$$

$$+ D_{W'_\infty}^{ACM}\frac{\delta W'_\infty}{\delta\rho(\mathbf{r})}$$

$$\tag{8}$$

where

$$D_{E_x}^{ACM} = \frac{\partial f^{ACM}}{\partial E_x}, \qquad D_{E_c^{GL2}}^{ACM} = \frac{\partial f^{ACM}}{\partial E_c^{GL2}} \tag{9}$$

$$D_{W_\infty}^{ACM} = \frac{\partial f^{ACM}}{\partial W_\infty}, \qquad D_{W'_\infty}^{ACM} = \frac{\partial f^{ACM}}{\partial W'_\infty} \tag{10}$$

and we used the short-hand notations

$$v_x(\mathbf{r}) = \frac{\delta E_x}{\delta \rho(\mathbf{r})}, \qquad v_c^{\mathrm{GL2}}(\mathbf{r}) = \frac{\delta E_c^{\mathrm{GL2}}}{\delta \rho(\mathbf{r})} \tag{11}$$

For the functionals not depending on W'_∞, i.e. SPL and LB, we have $D_{W'_\infty}^{\mathrm{ACM}} = 0$. The derivatives of eqs 9 and 10 are straightforward once the function f^{ACM} is fixed. The potentials $\delta W_\infty/\delta\rho$ and $\delta W'_\infty/\delta\rho$ depend on how the $\lambda \to \infty$ limit is treated. For the PC model, they are standard gradient expansion functional derivatives (see Appendix B). For the exact case, they can be computed by integrating the SCE force equation;[18,20,62] see the subsection on the Potentials for the Strong-Interaction Limit below.

Potentials for the Weak-Interaction Limit. The calculations of v_x and v_c^{GL2} require some attention. In this work we have used the optimized effective potential (OEP) method.[54,65] Then, the potential v_x or v_c^{GL2} (denoted with general notation v in eq 12) is given by the solution of the integral equation

$$\int \chi(\mathbf{r}, \mathbf{r}') v(\mathbf{r}') d\mathbf{r}' = \Lambda(\mathbf{r}) \tag{12}$$

where $\chi(\mathbf{r},\mathbf{r}')$ is the static linear-response function and

$$\Lambda(\mathbf{r}) = \sum_p \left[\int \phi_p(\mathbf{r}) \frac{\delta E}{\delta\phi_p(\mathbf{r})} \sum_{q\neq p} \frac{\phi_q(\mathbf{r})\phi_q(\mathbf{r}')}{\epsilon_p - \epsilon_q} d\mathbf{r}' + \frac{\delta E}{\delta\epsilon_p} \left| \phi_p(\mathbf{r}) \right|^2 \right] \tag{13}$$

with E being either the exact exchange or the second-order Görling-Levy correlation energies, and ϕ_p and ϵ_p being the Kohn−Sham orbitals and orbital energies, respectively. A similar approach was used in ref 7, leading to the fully self-consistent solution of double-hybrid functionals.

Computational Details. In our study we have considered several atoms, He, Be, Ne, and Ar, and the H$^-$ and F$^-$ ions, as well as the H$_2$ and N$_2$ molecules. For all these systems we have determined the self-consistent exact exchange orbitals and density. Then the GL2 correlation potential has been computed, on top of exact exchange orbitals, in a one-step nonself-consistent procedure. This was subsequently used to generate the ACM potentials.

Exact exchange potential calculations have been carried out with a locally modified version of the ACESII code.[66] The resulting exact exchange potentials are reported in the Supporting Information.[77] In order to solve the OEP equations and determine the exchange (and GL2) potentials, we have utilized the finite basis set implementation of the OEP method from refs 54 and 55 with a seed Slater potential[67] to ensure the stable and correct behavior of the exchange potentials in the asymptotic region. The same basis set has been used to expand both the orbitals and the exchange and correlation potentials. In particular, we have used an uncontracted cc-pVTZ basis set[68] for H$_2$ and N$_2$, a 20s10p2d basis set[69] for He, an uncontracted ROOS-ATZP basis set[70] for H, Be, Ne, and F, and for the Ar atom a modified basis set combining s- and p-type basis functions from the uncontracted ROOS-ATZP[70] with d- and f-type functions coming from the uncontracted aug-cc-pwCVQZ basis set.[53,71] The choice of the basis set was mostly dictated by the need to ensure the best possible expansion for both the wave functions and the OEP potential. We thus believe that the basis sets employed in this work provide a good compromise between an accurate description of the potential and the numerical stability of the computa-

tional procedure (see, for example, Figure S6[77]). For more details see refs 54 and 55.

Successively we have computed, in a post-SCF fashion, the XC potentials of the various ACM XC functionals (ISI,[15] revISI,[19] SPL,[17] and LB;[29] see Appendix A) using eq 8. Similarly we have computed, in a one-step procedure based on exact exchange orbitals, the GL2 potential as well as the other OEP correlation potentials (OEP2-sc, OEP2-SOSb). In all these potentials the single excited term has been neglected; anyway this is expected to yield a negligible effect on the final result.[54]

Potentials for the Strong-Interaction Limit. The exact (or very accurate[72]) functional derivative of $W_\infty[\rho]$ can be computed for spherically symmetric densities using the formalism and the procedure described in refs 18, 63, and 72. The potential is obtained by integrating numerically the force equation

$$\nabla v_{\mathrm{SCE}}[\rho](\mathbf{r}) = -\sum_{i=2}^{N} \frac{\mathbf{r} - \mathbf{f}_i(\mathbf{r}; [\rho])}{|\mathbf{r} - \mathbf{f}_i(\mathbf{r}; [\rho])|^3} \tag{14}$$

where the comotion functions $\mathbf{f}_i(\mathbf{r};[\rho])$, which are highly nonlocal density functionals, portray the strictly correlated regime, determining the positions of $N-1$ electrons as functions of the position $\mathbf{r}$ of one of them,[18,63,72] and the boundary condition $v_{\mathrm{SCE}}[\rho](|\mathbf{r}| \to \infty) = 0$ is used. Once v_{SCE} of eq 14 has been computed, we then have the exact relation[62,72]

$$\frac{\delta W_\infty[\rho]}{\delta\rho(\mathbf{r})} \equiv v_{xc}^\infty(\mathbf{r}) = v_{\mathrm{SCE}}(\mathbf{r}) - v_{\mathrm{H}}(\mathbf{r}) \tag{15}$$

where $v_{\mathrm{H}}(\mathbf{r})$ is the Hartree potential.

We have computed $v_{xc}^\infty(\mathbf{r})$ of eqs 14 and 15 for H$^-$, Be, and Ne, for the same densities as described in the Computational Details section, using the comotion functions described in refs 18, 63, and 72, which are exact for $N = 2$ and very accurate (or exact) for $N > 2$.[72] Moreover, even when these comotion functions are not optimal, the functional derivative of the corresponding $W_\infty[\rho]$ still obeys eqs 14 and 15.[72]

In Figure 1, we compare these exact (or very accurate) $v_{xc}^\infty(\mathbf{r})$ with the functional derivative of $W_\infty^{\mathrm{PC}}[\rho]$ for the three species. We see that, as anticipated, since the PC model is a GEA, it diverges at large internuclear distances, tending to minus infinity (see Appendix B for more details), a feature that would further prevent the performing of self-consistent calculations. The exact $v_{xc}^\infty(\mathbf{r})$, instead, displays the correct asymptotic behavior $\propto -1/r$.[18,62] Nonetheless, we see that in the region where the density is significantly different from zero, the PC model provides a very decent approximation to the exact $v_{xc}^\infty(\mathbf{r})$. In the next sections, we will then use the much cheaper PC potentials, since we will always compute them on a reference density, where they seem to give rather reasonable results (with the exception of the region close and far from the nucleus). This choice has been further validated by comparing for a few cases the potentials obtained from the SPL and LB models using the PC and SCE functional derivatives: in all cases the differences between the two have been found to be very small, of course with the exception of the asymptotic region far from the nucleus.

There is at present no exact result available for the functional derivative of the zero-point term $W'_\infty[\rho]$, which is the object of an ongoing investigation. For this reason, we will use again the PC model, which also yields a potential that diverges, this
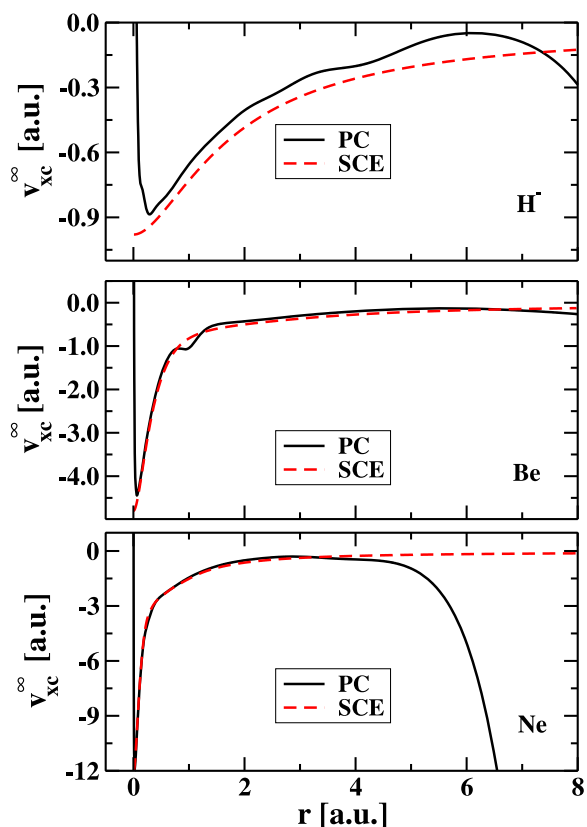
Figure 1. Comparison between the exact (or very accurate) functional derivative of the leading term $W_\infty[\rho]$ in eq 3, computed with the strictly correlated electrons (SCE) formalism of eqs 14 and 15,[18,63,72] and the functional derivative of the GEA approximation obtained from the PC model of eq 5.

time going to plus infinity, but only rather far from the nucleus (see Figure 2 and Appendix B for more details).

■ RESULTS

In Figure 3 we show the correlation potentials corresponding to different XC functionals (on the scale of the plot ISI and revISI are hardly distinguishable; therefore, only the ISI curve
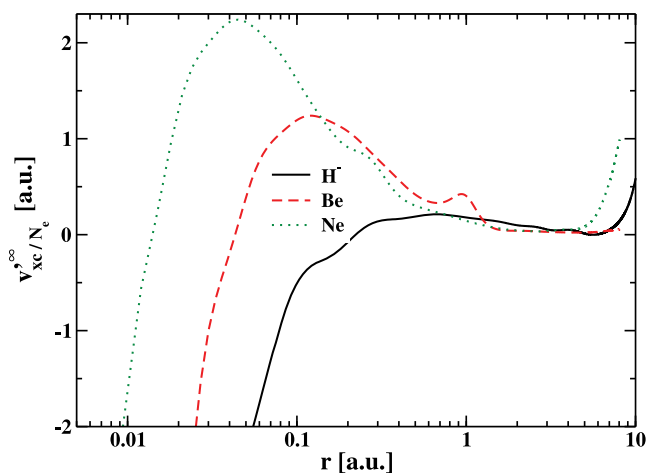
Figure 2. Functional derivative of $W'_\infty[\rho]$, divided by the number of electrons, obtained using the GEA approximation based on the PC model of eq 6, for several atoms.
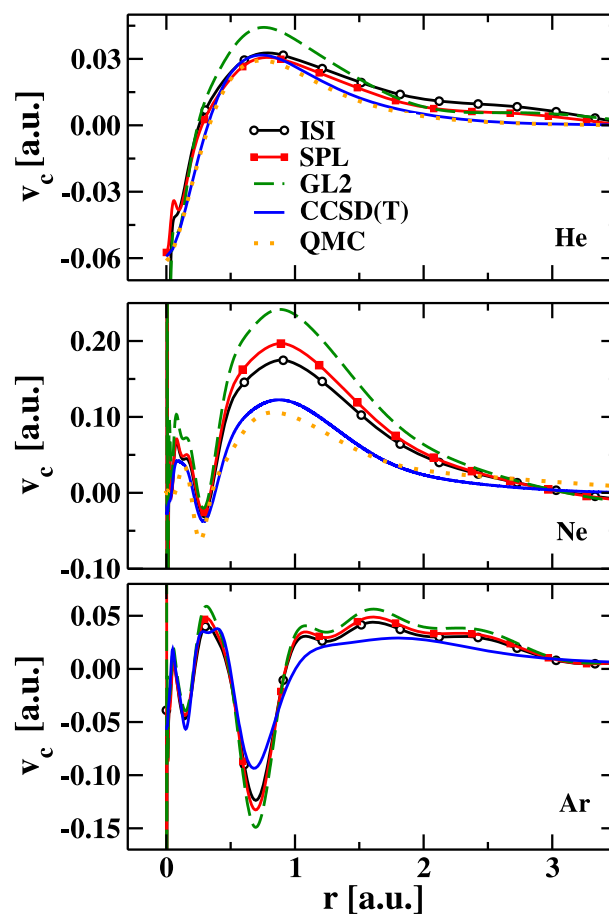
Figure 3. Correlation potentials obtained with different methods for several atoms.

has been shown; the same applies to SPL and LB.). We recall that all the methods considered in this work include the exchange contribution exactly; therefore, only the correlation part of the potential ($v_c^{ACM} = v_{xc}^{ACM} - v_x$) is of interest for an assessment of the methods. For comparison we have also reported the correlation potential obtained via direct inversion of the coupled cluster single double with perturbative triple (CCSD(T)) density[73] as well as the one obtained from quantum Monte Carlo (QMC) calculations.[74,75] Both potentials are very accurate and are assumed here as benchmark references. Note anyway that these potentials do not stem from the exact exchange densities used to generate the ACMs potentials but correspond to self-consistent CCSD(T) or QMC densities. Nevertheless, we expect the difference due to this issue to be almost negligible for the purpose of this work.

The plots of Figure 3 show that, in all cases, the various potentials have quite similar shapes. This indicates that for all the ACMs the correlation potential is physically meaningful and describes the main features of the exact potential. Moreover, the ACMs potentials are generally closer to the reference ones than GL2. This latter situation can be measured quantitatively considering the integral error

$$\Delta v_c^{ACM} = \int \rho(\mathbf{r})|v_c^{ACM}(\mathbf{r}) - v_c^{Ref}(\mathbf{r})|d\mathbf{r} \tag{16}$$

where we use the CCSD(T) potential as reference (*Ref*), and ρ is the exact exchange self-consistent density (i.e., the one used to compute v_c^{ACM}). The corresponding values are reported in

Table 1, whereas a plot of the integrands for the Ne atom case is shown in Figure 4. These data confirm that the ACMs

Table 1. Integral Error (Δv_c^{ACM}; See Eq 16) for Different Potentials

	He	Ne	Ar
ISI	0.0088	0.3734	0.1718
revISI	0.0113	0.3136	0.1583
SPL	0.0060	0.5083	0.2123
LB	0.0070	0.5778	0.2258
GL2	0.0212	0.8151	0.2886
OEP2-sc	0.0133	0.1900	0.1062
OEP2-SOSb	0.0170	0.2140	0.1710
OEP2-SOS(opt)	0.0102	0.1127	0.2339
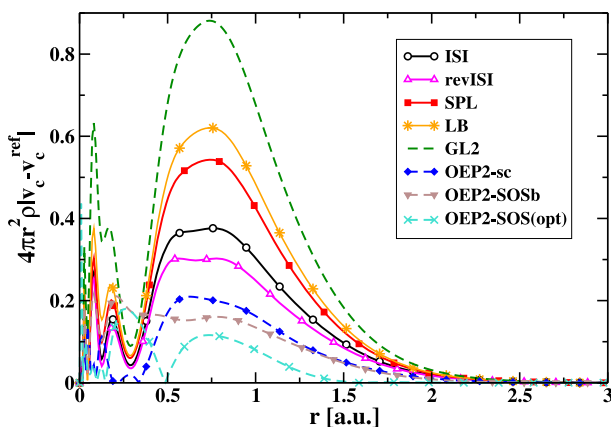
Figure 4. Radial density-weighted absolute errors (see the integrand of eq 16) for various potentials based on adiabatic connection models as well as for GL2 and several second-order OEP potentials, in the case of Ne atom.

provide a significant improvement over GL2, yielding values of Δv_c^{ACM} that are in most cases almost one-half those of GL2. Moreover, Table 1 reports also the integral errors for some accurate second-order OEP methods, namely OEP2-sc,[8,10] OEP2-SOSb,[54,55] and OEP2-SOS(opt),[55] indicating that the ACMs potentials are competitive with the best available OEP methods. Finally, we find that in general ISI and revISI are slightly better than SPL and LB, most probably due to inclusion of the zero-point term $W'_\infty[\rho]$.

An additional indication of the quality of the ACMs potentials can come by the analysis of the effect they have on the Kohn−Sham orbital energies. In particular, we have considered the first-order perturbative variation of the energy of the highest occupied molecular orbital (HOMO), i.e.

$\langle H|v_c^{AMC}|H\rangle$ with $|H\rangle$ being the HOMO state, due to the application of the potential v_c^{AMC}. These data are reported in Table 2 together with some reference values. These results confirm the trends observed for the Δv_c^{ACM}, showing that all the ACMs potentials yield HOMO energy variations in line with OEP2-sc and OEP2-SOSb and close to the reference values; on the other hand, GL2 yields quite overestimated HOMO energy variations.

We remark that the improvement found for the ACMs with respect to GL2 is particularly significant because it mainly corresponds to a reduction of the GL2 overestimation of the potential in the outer valence region. This feature is in fact one of the main limitations that GL2 experiences in OEP Kohn−Sham calculations, which leads to several problems including, sometimes, the impossibility to converge OEP-GL2 Kohn−Sham self-consistent calculations. Indeed, several modifications of OEP-GL2, such as OEP2-sc, OEP2-SOSb, and OEP2-SOS(opt), have been developed to account for this problem.[8,53−55,76] Thus, the partial correction of this drawback from the ACMs is a very promising feature of these functionals which allows them to yield potentials close to the accurate OEP ones (see Figure S1[77] where we compare, for the Ne atom, ISI and SPL with OEP2-sc, OEP2-SOSb, and OEP2-SOS(opt) as well as with OEP-ccpt2[10]).

As a further example we consider the case of the beryllium atom which is known to be a rather extreme case where the GL2 potential performs poorly, overestimating the correct correlation potential, such that self-consistent OEP-GL2 calculations fail to converge. Thus, in Figure 5 we report the
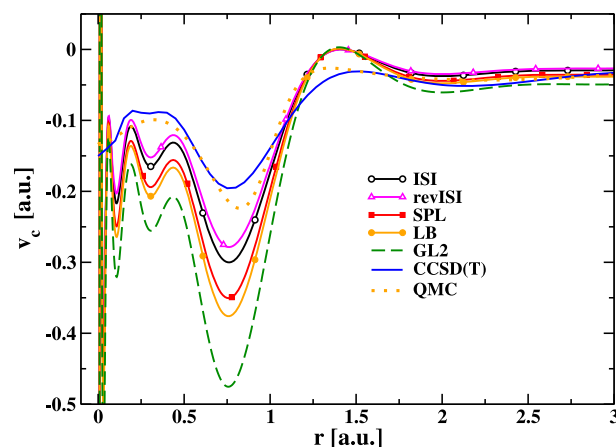
Figure 5. Correlation potentials obtained with different methods for the beryllium atom.

various correlation potentials computed for beryllium (in Figure S2[77] we report also the accurate second-order OEP

Table 2. First-Order Variation of the Energy (eV) of the Kohn-Sham Highest Occupied Molecular Orbital (HOMO) as Due to the Application of Different Correlation Potentials[a]

	$\langle H|v_c^{AMC}|H\rangle$					$\epsilon_H - \epsilon_H^{OEPx}$			
	ISI	revISI	SPL	LB	GL2	GL2	OEP2-sc	OEP2-SOSb	ref
He	0.576	0.610	0.505	0.551	0.746	0.751	0.427	0.547	0.419
Ne	3.211	3.026	3.627	3.826	4.528	5.491	3.012	2.416	1.935
Ar	0.573	0.538	0.652	0.680	0.767	1.137	0.740	0.558	0.672

[a]The right part of the table reports, for comparison, the difference between the self-consistent HOMO energy computed with some correlated methods and the one obtained at the exact exchange level ($\epsilon_H - \epsilon_H^{OEPx}$). Reference values are obtained from inverted CCSD(T) calculations.

potentials for comparison). Inspection of the plots shows that also in this difficult case the ACMs potentials, especially ISI and revISI, improve substantially over GL2 being comparable to the OEP2-SOSb and OEP2-SOS(opt) approaches. Note also that the accurate OEP2-sc method instead yields an underestimation (in absolute values) of the correlation potential of the beryllium atom.

The analysis discussed above, evidenced the similarity of the ACMs potentials with scaled GL2 ones.[53−55] This finding is not completely surprising if we inspect the magnitudes of the different contributions forming the ACM potential in eq 8, i.e. $D_{E_x}^{ACM}$, $D_{E_c^{GL2}}^{ACM}$, $D_{W_\infty}^{ACM}$, and $D_{W'_\infty}^{ACM}$ (see Table 3). The data show in

Table 3. Values of the Partial Derivatives Appearing in Eq 8 for the Various ACM Correlation Functionals of Different Atoms

|		$D_{E_x}^{ACM} - 1$	$D_{E_c^{GL2}}^{ACM}$	$D_{W_\infty}^{ACM}$	$D_{W'_\infty}^{ACM}$
He	ISI	−0.029	0.642	0.029	0.006
	revISI	−0.036	0.615	0.036	0.009
	SPL	−0.014	0.699	0.014	
	LB	−0.012	0.757	0.012	
Be	ISI	−0.030	0.617	0.030	0.005
	revISI	−0.038	0.570	0.038	0.007
	SPL	−0.011	0.726	0.011	
	LB	−0.009	0.782	0.009	
Ne	ISI	−0.014	0.724	0.014	0.002
	revISI	−0.018	0.683	0.018	0.003
	SPL	−0.005	0.819	0.005	
	LB	−0.004	0.869	0.004	
Ar	ISI	−0.007	0.079	0.007	0.001
	revISI	−0.010	0.751	0.010	0.001
	SPL	−0.002	0.873	0.002	
	LB	−0.002	0.904	0.002	

fact that the main contribution to the potential of any of the ACMs is a scaled GL2 component, with a magnitude of about 70%. This finding traces back to the fact that the ACMs are effectively all-order renormalizations of the density functional perturbation theory,[15] thus they basically perform a "rescaling" of the GL2 correlation contribution. This feature puts these potentials not only in relation with the spin-opposite-scaled OEP methods (OEP2-SOS), as mentioned above, but also with the recently developed self-consistent OEP double-hybrid[7] method, which also shows a similar signature. Then, the success of the later methods in self-consistent calculations can be considered as a promising indicator for the quality of the ACM potentials and the possible success of future self-consistent calculations based on the ACM functionals.

We remark anyway that, despite the scaled GL2 being the main component of the correlation potential of ACMs, other contributions may also be present with a non-negligible effect. This can be seen, for example, in Figure 6 where we plot the quantity $v_c^{ACM} - D_{E_c^{GL2}}^{ACM} v_c^{GL2}$ for the Ne atom. The plot shows that all the ACM potentials show relevant features in the core regions (i.e., $v_c^{ACM} - D_{E_c^{GL2}}^{ACM} v_c^{GL2} \neq 0$), that possibly originate from the larger correlation effects felt by core electrons, implying a larger contribution from the $D_{W_\infty}^{ACM}$ component (see also the subsection Potentials for the Strong-Interaction Limit). This is more evident for ISI and revISI, whereas the SPL and LB correlation potentials are slightly closer to scaled GL2 potentials.
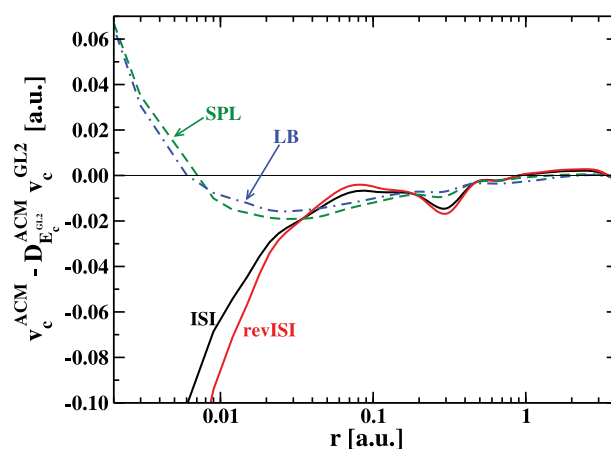
Figure 6. Difference between the correlation potentials of various adiabatic connection models and the scaled second-order Görling Levy correlation potential ($v_c^{ACM} - D_{E_c^{GL2}}^{ACM} v_c^{GL2}$) for the neon atom.

It is worth noting also that the "renormalization" effect of the ACM correlation potentials will increase when systems with stronger correlation are considered. Unfortunately, for such systems the OEP equation needed to generate the GL2 potential cannot be generally solved; thus we had to limit our investigation only to the simple case of the F$^-$ anion, to be compared with the Ne atom. This comparison is shown in Figure 7 for the case of the revISI correlation potential (other
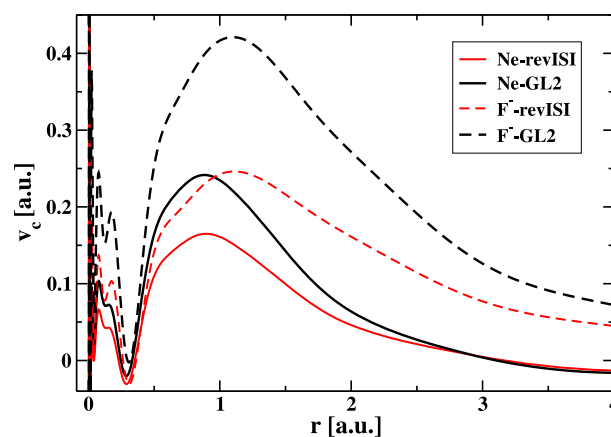
Figure 7. GL2 and revISI correlation potentials for the Ne atom and the F$^-$ anion.

ACMs behave similarly). From the plot it can be seen that for the F$^-$ anion, where correlation effects are slightly larger than in Ne, indeed a greater difference between the revISI and the GL2 potentials is found. This fact is also confirmed by the computed value of $D_{E_c^{GL2}}^{ACM}$ that for F$^-$ is 0.583 (to be compared with 0.683 in Ne, see Table 3); note also that $D_{W_\infty}^{ACM}$ is 0.030 for F$^-$, while it is 0.018 for the neon atom.

To conclude, in Figure 8 we report the correlation potentials computed for two simple molecules, namely H$_2$ and N$_2$. In these cases we have also used as a reference the correlated potential obtained from relaxed CCSD(T) density observing the same qualitative behavior as already found in atoms except for some oscillations in the asymptotic region due to basis set issues in the OEP calculation of v_c^{GL2}. Thus, all the ACMs provide a reduction of the correlation potential with respect to GL2. In particular, ISI and revISI (not shown because it is very
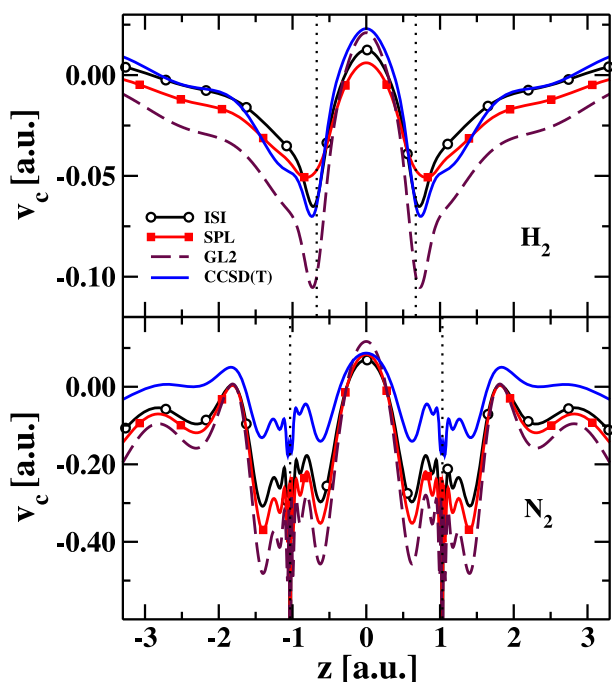
Figure 8. Correlation potentials of different adiabatic connection models as well as of the second-order Görling-Levy (GL2) correlation for the H_2 (top) and N_2 (bottom) molecules, plotted along the bond axis. The vertical lines indicate the positions of the atoms in each molecule.

similar to ISI) provide a slightly larger reduction than SPL and LB (not shown because it is very close to SPL). Also here the direct comparison with several correlated OEP potentials made for nitrogen dimer (Figure S3[77]) reveals a remarkably good performance for all ACMs. The ISI and SPL give almost the same potentials as OEP2-sc which is considered as the state-of-the-art correlated OEP method.

CONCLUSIONS

We have studied the correlation potentials produced by different adiabatic connection models to investigate whether these methods are able to produce, besides reasonable energies,[31−33] also physically meaningful potentials. This is, in fact, a fundamental issue in view of a possible future use of the ACMs in self-consistent calculations.

Our results showed that indeed all the investigated functionals are able to provide rather accurate correlation potentials, with ISI and revISI being slightly superior to SPL and LB. In particular, all the considered correlation potentials display the correct features of the exact correlation potential and reduce the overestimation behavior which is typical of the GL2 method.[8,78] Thus, all in all, the ACM-based correlation potentials are comparable to those produced by some state-of-the-art optimized effective potential methods (OEP2-sc,[8,10] OEP2-SOS[54,55]).

These results suggest that it might be worth pursuing the realization of self-consistent calculations using the ACM XC functionals, which would provide a final assessment of their quality. However, to reach this goal a few issues need first to be solved. In particular, one needs to develop proper density functionals for the $\lambda \to \infty$ limit, in order to replace the gradient expansions of eqs 5 and 6, which lead to divergences in the potential. The functionals of refs 25−27 are already very

good candidates, although they pose new technical problems at the implementation level due to their nonlocal density dependence. If one wants to stay within gradient approximations, then the PC GEA should be renormalized into GGAs. Moreover, a proper OEP scheme, similar to the one used for the implementation of self-consistent double hybrids,[7] needs to be implemented to deal with the various terms appearing in eq 8, which are both of implicit nonlocal and explicit semilocal types. In addition, several numerical issues would need to be taken into account, such as the stability of the self-consistent solution with respect to the basis set and the influence of the accuracy of the potential on the correlation energy.

APPENDIX A: ADIABATIC CONNECTION MODELS

In this work we consider several ACMs. They main features of each one are described below.

ISI Functional.[15] The XC energy is

$$E_{xc}^{ISI} = W_\infty + \frac{2X}{Y}\left[\sqrt{1 + Y} - 1 - Z \ln\left(\frac{\sqrt{1+Y}+Z}{1+Z}\right)\right] \tag{17}$$

with

$$X = \frac{xy^2}{z^2}, \quad Y = \frac{x^2y^2}{z^4}, \quad Z = \frac{xy^3}{z^3} - 1 \tag{18}$$

$$x = -4E_c^{GL2}, \quad y = W'_\infty, \quad z = E_x - W_\infty \tag{19}$$

revISI Functional.[19] The XC energy is

$$E_{xc}^{revISI} = W_\infty + \frac{b}{\sqrt{1+c}+d} \tag{20}$$

with

$$b = -\frac{8E_c^{GL2}(W'_\infty)^2}{(E_x - W_\infty)^2} \tag{21}$$

$$c = \frac{16(E_c^{GL2}W'_\infty)^2}{(E_x - W_\infty)^4} \tag{22}$$

$$d = -1 - \frac{8E_c^{GL2}(W'_\infty)^2}{(E_x - W_\infty)^3} \tag{23}$$

SPL Functional.[17] The XC energy is

$$E_{xc}^{SPL} = E_x + (E_x - W_\infty)\left[\frac{\sqrt{1+2\chi}-1-\chi}{\chi}\right] \tag{24}$$

with

$$\chi = \frac{2E_c^{GL2}}{W_\infty - E_x} \tag{25}$$

LB Functional.[29] The XC energy is

$$E_{xc}^{LB} = E_x + \frac{2b}{c}\left[\sqrt{1+c} - \frac{1+c/2}{1+c} - c\right] \tag{26}$$

with

$$b = \frac{E_x - W_\infty}{2}, \quad c = \frac{8E_c^{GL2}}{5(W_\infty - E_x)} \tag{27}$$

■ APPENDIX B: FUNCTIONAL DERIVATIVE OF THE PC FUNCTIONALS

The functional derivative of eqs 5 and 6 with respect to the density is

$$\frac{\delta W_\infty^{PC}[\rho]}{\delta \rho(\mathbf{r})} = \frac{4A}{3}\rho(\mathbf{r})^{1/3} - 2B\frac{\nabla^2\rho(\mathbf{r})}{\rho(\mathbf{r})^{4/3}} + \frac{4B}{3}\frac{|\nabla\rho(\mathbf{r})|^2}{\rho(\mathbf{r})^{7/3}}$$

(28)

$$\frac{\delta W_\infty'^{PC}[\rho]}{\delta \rho(\mathbf{r})} = \frac{3C}{2}\rho(\mathbf{r})^{1/2} - 2D\frac{\nabla^2\rho(\mathbf{r})}{\rho(\mathbf{r})^{7/6}} + \frac{7D}{6}\frac{|\nabla\rho(\mathbf{r})|^2}{\rho(\mathbf{r})^{13/6}}$$

(29)

In order to study which terms are responsible for the divergence observed (see the subsection Potentials for the Strong-Interaction Limit), we consider the asymptotic expression[79] for a density of N electrons bound by a total positive charge Z, with $r = |\mathbf{r}|$

$$\rho(r \to \infty) \sim r^\beta e^{-\alpha r}$$

(30)

with $\alpha = 2\sqrt{2I}$, $\beta = \frac{Z-N+1}{\sqrt{2I}} - 1$, and I being the first ionization potential (e.g., for the Ne atom $\alpha \approx 2.5$ and $\beta \approx -0.2$). By plugging eq 30 into eq 28, one sees that the second and third terms go to leading order like $r^{-\frac{\beta}{3}}e^{\frac{\alpha}{3}r}$; however, the second term is multiplied by a negative constant, namely $-2B$, which determines the divergence to $-\infty$ over the third term, whose prefactor is $\frac{4B}{3}$. Analogously, for eq 29, one sees that the second and third terms, again, diverge with the same leading order, which, in this case, is $r^{-\frac{\beta}{6}}e^{\frac{\alpha}{6}r}$. In this latter case, however, the second term is multiplied by the positive constant $-2D$, which determines the divergence to $+\infty$ over the third term, whose prefactor is $\frac{7D}{6}$. Since all the ACM potentials calculated in this work make use of the PC approximation for the strong-interaction limit terms, they all show a negative divergence, appearing "earlier" in the SPL and LB than in the ISI and revISI models (as these latter also include the ingredient $\frac{\delta W_\infty'^{PC}[\rho]}{\delta \rho(\mathbf{r})}$, which partially compensates the asymptotically dominant term). Moreover, while this analysis applies to the exact asymptotic density behavior, the use of Gaussian basis sets worsens the divergence at large r.

■ ASSOCIATED CONTENT

⑤ Supporting Information

The Supporting Information is available free of charge on the ACS Publications website at DOI: 10.1021/acs.jctc.8b01037.

> Correlation potentials of Ne and Be atoms and N_2 dimer, exchange potentials of atoms and molecules, plot of the ISI correlation potential of H_2 as computed with different basis sets (PDF)

■ AUTHOR INFORMATION

Corresponding Author

*E-mail: eduardo.fabiano@cnr.it.

ORCID ⓘ

Eduardo Fabiano: 0000-0002-3990-669X
Szymon Śmiga: 0000-0002-5941-5409
Fabio Della Sala: 0000-0003-0940-8830
Ireneusz Grabowski: 0000-0002-5661-5659

Paola Gori-Giorgi: 0000-0002-5952-1172

Notes

The authors declare no competing financial interest.

■ REFERENCES

(1) Scuseria, G. E.; Staroverov, V. N. In *Theory and Applications of Computational Chemistry: The First Forty Years*; Dykstra, C. E., Frenking, G., Kim, K. S., Scuseria, G. E., Eds.; Elsevier: Amsterdam, 2005.

(2) Della Sala, F.; Fabiano, E.; Constantin, L. A. Kinetic-energy-density dependent semilocal exchange-correlation functionals. *Int. J. Quantum Chem.* **2016**, *116*, 1641−1694.

(3) Perdew, J. P.; Schmidt, K. Jacob's ladder of density functional approximations for the exchange-correlation energy. *AIP Conf. Proc.* **2000**, *577*, 1−20.

(4) Jiang, H.; Engel, E. Random-phase-approximation-based correlation energy functionals: Benchmark results for atoms. *J. Chem. Phys.* **2007**, *127*, 184108.

(5) Chen, G. P.; Voora, V. K.; Agee, M. M.; Balasubramani, S. G.; Furche, F. Random-Phase Approximation Methods. *Annu. Rev. Phys. Chem.* **2017**, *68*, 421−445.

(6) Grimme, S. Semiempirical hybrid density functional with perturbative second-order correlation. *J. Chem. Phys.* **2006**, *124*, 034108.

(7) Śmiga, S.; Franck, O.; Mussard, B.; Buksztel, A.; Grabowski, I.; Luppi, E.; Toulouse, J. Self-consistent double-hybrid density-functional theory using the optimized-effective-potential method. *J. Chem. Phys.* **2016**, *145*, 144102.

(8) Bartlett, R. J.; Grabowski, I.; Hirata, S.; Ivanov, S. The exchange-correlation potential in ab initio density functional theory. *J. Chem. Phys.* **2005**, *122*, 034104.

(9) Bartlett, R. J.; Lotrich, V. F.; Schweigert, I. V. Ab initio density functional theory: The best of both worlds? *J. Chem. Phys.* **2005**, *123*, 062205.

(10) Grabowski, I.; Lotrich, V.; Bartlett, R. J. Ab initio density functional theory applied to quasidegenerate problems. *J. Chem. Phys.* **2007**, *127*, 154111.

(11) Harris, J.; Jones, R. O. The surface energy of a bounded electron gas. *J. Phys. F: Met. Phys.* **1974**, *4*, 1170.

(12) Langreth, D.; Perdew, J. P. The exchange-correlation energy of a metallic surface. *Solid State Commun.* **1975**, *17*, 1425−1429.

(13) Gunnarsson, O.; Lundqvist, B. I. Exchange and correlation in atoms, molecules, and solids by the spin-density-functional formalism. *Phys. Rev. B* **1976**, *13*, 4274−4298.

(14) Savin, A.; Colonna, F.; Pollet, R. Adiabatic connection approach to density functional theory of electronic systems. *Int. J. Quantum Chem.* **2003**, *93*, 166−190.

(15) Seidl, M.; Perdew, J. P.; Kurth, S. Simulation of All-Order Density-Functional Perturbation Theory, Using the Second Order and the Strong-Correlation Limit. *Phys. Rev. Lett.* **2000**, *84*, 5070−5073.

(16) Görling, A.; Levy, M. Exact Kohn-Sham scheme based on perturbation theory. *Phys. Rev. A: At., Mol., Opt. Phys.* **1994**, *50*, 196−204.

(17) Seidl, M.; Perdew, J. P.; Levy, M. Strictly correlated electrons in density-functional theory. *Phys. Rev. A: At., Mol., Opt. Phys.* **1999**, *59*, 51.

(18) Seidl, M.; Gori-Giorgi, P.; Savin, A. Strictly correlated electrons in density-functional theory: A general formulation with applications

to spherical densities. *Phys. Rev. A: At., Mol., Opt. Phys.* **2007**, *75*, 042511.

(19) Gori-Giorgi, P.; Vignale, G.; Seidl, M. Electronic Zero-Point Oscillations in the Strong-Interaction Limit of Density Functional Theory. *J. Chem. Theory Comput.* **2009**, *5*, 743−753.

(20) Malet, F.; Mirtschink, A.; Cremon, J. C.; Reimann, S. M.; Gori-Giorgi, P. Kohn-Sham density functional theory for quantum wires in arbitrary correlation regimes. *Phys. Rev. B: Condens. Matter Mater. Phys.* **2013**, *87*, 115146.

(21) Lewin, M. Semi-classical limit of the Levy-Lieb functional in Density Functional Theory. *Comptes Rendus Mathematique* **2018**, *356*, 449−455.

(22) Cotar, C.; Friesecke, G.; Klüppelberg, C. Smoothing of transport plans with fixed marginals and rigorous semiclassical limit of the Hohenberg-Kohn functional. *Arch. Ration. Mech. Anal.* **2018**, *228*, 891−922.

(23) Grossi, J.; Kooi, D. P.; Giesbertz, K. J. H.; Seidl, M.; Cohen, A. J.; Mori-Sánchez, P.; Gori-Giorgi, P. Fermionic Statistics in the Strongly Correlated Limit of Density Functional Theory. *J. Chem. Theory Comput.* **2017**, *13*, 6089−6100.

(24) Seidl, M.; Perdew, J. P.; Kurth, S. Density functionals for the strong-interaction limit. *Phys. Rev. A: At., Mol., Opt. Phys.* **2000**, *62*, 012502.

(25) Wagner, L. O.; Gori-Giorgi, P. Electron avoidance: A nonlocal radius for strong correlation. *Phys. Rev. A: At., Mol., Opt. Phys.* **2014**, *90*, 052512.

(26) Bahmann, H.; Zhou, Y.; Ernzerhof, M. The shell model for the exchange-correlation hole in the strong-correlation limit. *J. Chem. Phys.* **2016**, *145*, 124104.

(27) Vuckovic, S.; Gori-Giorgi, P. Simple Fully Nonlocal Density Functionals for Electronic Repulsion Energy. *J. Phys. Chem. Lett.* **2017**, *8*, 2799−2805.

(28) Seidl, M.; Perdew, J. P.; Kurth, S. Erratum: Density functionals for the strong-interaction limit [Phys. Rev. A 62, 012502 (2000)]. *Phys. Rev. A: At., Mol., Opt. Phys.* **2005**, *72*, 029904.

(29) Liu, Z.-F.; Burke, K. Adiabatic connection in the low-density limit. *Phys. Rev. A: At., Mol., Opt. Phys.* **2009**, *79*, 064503.

(30) Ernzerhof, M. Construction of the adiabatic connection. *Chem. Phys. Lett.* **1996**, *263*, 499−506.

(31) Fabiano, E.; Gori-Giorgi, P.; Seidl, M.; Della Sala, F. Interaction-Strength Interpolation Method for Main-Group Chemistry: Benchmarking, Limitations, and Perspectives. *J. Chem. Theory Comput.* **2016**, *12*, 4885−4896.

(32) Giarrusso, S.; Gori-Giorgi, P.; Della Sala, F.; Fabiano, E. Assessment of interaction-strength interpolation formulas for gold and silver clusters. *J. Chem. Phys.* **2018**, *148*, 134106.

(33) Vuckovic, S.; Gori-Giorgi, P.; Della Sala, F.; Fabiano, E. Restoring Size Consistency of Approximate Functionals Constructed from the Adiabatic Connection. *J. Phys. Chem. Lett.* **2018**, *9*, 3137.

(34) Jankowski, K.; Grabowski, I.; Nowakowski, K.; Wasilewski, J. Ab initio Correlation Effects in Density Functional Theories: An Electron-Distribution-Based Study for Neon. *Collect. Czech. Chem. Commun.* **2005**, *70*, 1157−1176.

(35) Fabiano, E.; Della Sala, F. Localized exchange-correlation potential from second-order self-energy for accurate Kohn-Sham energy gap. *J. Chem. Phys.* **2007**, *126*, 214102.

(36) Grabowski, I.; Teale, A. M.; Śmiga, S.; Bartlett, R. J. Comparing ab initio density-functional and wave function theories: The impact of correlation on the electronic density and the role of the correlation potential. *J. Chem. Phys.* **2011**, *135*, 114111.

(37) Grabowski, I.; Teale, A. M.; Fabiano, E.; Śmiga, S.; Buksztel, A.; Della Sala, F. A density difference based analysis of orbital-dependent exchange-correlation functionals. *Mol. Phys.* **2014**, *112*, 700−710.

(38) Buijse, M. A.; Baerends, E. J.; Snijders, J. G. Analysis of correlation in terms of exact local potentials: Applications to two-electron systems. *Phys. Rev. A: At., Mol., Opt. Phys.* **1989**, *40*, 4190−4202.

(39) Umrigar, C. J.; Gonze, X. Accurate exchange-correlation potentials and total-energy components for the helium isoelectronic series. *Phys. Rev. A: At., Mol., Opt. Phys.* **1994**, *50*, 3827−3837.

(40) Gritsenko, O.; van Leeuwen, R.; Baerends, E. J. Analysis of electron interaction and atomic shell structure in terms of local potentials. *J. Chem. Phys.* **1994**, *101*, 8955.

(41) Filippi, C.; Gonze, X.; Umrigar, C. J. In *Recent developments and applications in modern DFT*; Seminario, J. M., Ed.; Elsevier: Amsterdam, 1996; pp 295−321.

(42) Baerends, E. J.; Gritsenko, O. V. Effect of molecular dissociation on the exchange-correlation Kohn-Sham potential. *Phys. Rev. A: At., Mol., Opt. Phys.* **1996**, *54*, 1957−1972.

(43) Gritsenko, O. V.; van Leeuwen, R.; Baerends, E. J. Molecular exchange-correlation Kohn-Sham potential and energy density from ab initio first- and second-order density matrices: Examples for XH (X= Li, B, F). *J. Chem. Phys.* **1996**, *104*, 8535−8545.

(44) Tempel, D. G.; Martínez, T. J.; Maitra, N. T. Revisiting Molecular Dissociation in Density Functional Theory: A Simple Model. *J. Chem. Theory Comput.* **2009**, *5*, 770−780.

(45) Helbig, N.; Tokatly, I. V.; Rubio, A. Exact Kohn-Sham potential of strongly correlated finite systems. *J. Chem. Phys.* **2009**, *131*, 224105.

(46) Ryabinkin, I. G.; Kohut, S. V.; Staroverov, V. N. Reduction of electronic wave functions to Kohn-Sham effective potentials. *Phys. Rev. Lett.* **2015**, *115*, 083001.

(47) Ospadov, E.; Ryabinkin, I. G.; Staroverov, V. N. Improved method for generating exchange-correlation potentials from electronic wave functions. *J. Chem. Phys.* **2017**, *146*, 084103.

(48) Kohut, S. V.; Polgar, A. M.; Staroverov, V. N. Origin of the step structure of molecular exchange-correlation potentials. *Phys. Chem. Chem. Phys.* **2016**, *18*, 20938−20944.

(49) Hodgson, M. J. P.; Ramsden, J. D.; Godby, R. W. Origin of static and dynamic steps in exact Kohn-Sham potentials. *Phys. Rev. B: Condens. Matter Mater. Phys.* **2016**, *93*, 155146.

(50) Ying, Z. J.; Brosco, V.; Lopez, G. M.; Varsano, D.; Gori-Giorgi, P.; Lorenzana, J. Anomalous scaling and breakdown of conventional density functional theory methods for the description of Mott phenomena and stretched bonds. *Phys. Rev. B: Condens. Matter Mater. Phys.* **2016**, *94*, 075154.

(51) Benítez, A.; Proetto, C. R. Kohn-Sham potential for a strongly correlated finite system with fractional occupancy. *Phys. Rev. A: At., Mol., Opt. Phys.* **2016**, *94*, 052506.

(52) Ryabinkin, I. G.; Ospadov, E.; Staroverov, V. N. Exact exchange-correlation potentials of singlet two-electron systems. *J. Chem. Phys.* **2017**, *147*, 164117.

(53) Grabowski, I.; Fabiano, E.; Della Sala, F. Optimized effective potential method based on spin-resolved components of the second-order correlation energy in density functional theory. *Phys. Rev. B: Condens. Matter Mater. Phys.* **2013**, *87*, 075103.

(54) Grabowski, I.; Fabiano, E.; Teale, A. M.; Śmiga, S.; Buksztel, A.; Della Sala, F. Orbital-dependent second-order scaled-opposite-spin correlation functionals in the optimized effective potential method. *J. Chem. Phys.* **2014**, *141*, 024113.

(55) Śmiga, S.; Della Sala, F.; Buksztel, A.; Grabowski, I.; Fabiano, E. Accurate Kohn-Sham ionization potentials from scaled-opposite-spin second-order optimized effective potential methods. *J. Comput. Chem.* **2016**, *37*, 2081−2090.

(56) Medvedev, M. G.; Bushmarinov, I. S.; Sun, J.; Perdew, J. P.; Lyssenko, K. A. Density functional theory is straying from the path toward the exact functional. *Science* **2017**, *355*, 49−52.

(57) Brorsen, K. R.; Yang, Y.; Pak, M. V.; Hammes-Schiffer, S. Is the Accuracy of Density Functional Theory for Atomization Energies and Densities in Bonding Regions Correlated? *J. Phys. Chem. Lett.* **2017**, *8*, 2076−2081.

(58) Korth, M. Density Functional Theory: Not Quite the Right Answer for the Right Reason Yet. *Angew. Chem., Int. Ed.* **2017**, *56*, 5396−5398.

(59) Mezei, P. D.; Csonka, G. I.; Kállay, M. Electron Density Errors and Density-Driven Exchange-Correlation Energy Errors in Approx-

imate Density Functional Calculations. *J. Chem. Theory Comput.* **2017**, *13*, 4753−4764.

(60) Della Sala, F.; Fabiano, E.; Constantin, L. A. Kohn-Sham kinetic energy density in the nuclear and asymptotic regions: Deviations from the von Weizsäcker behavior and applications to density functionals. *Phys. Rev. B: Condens. Matter Mater. Phys.* **2015**, *91*, 035126.

(61) Constantin, L. A.; Fabiano, E.; Pitarke, J. M.; Della Sala, F. Semilocal density functional theory with correct surface asymptotics. *Phys. Rev. B: Condens. Matter Mater. Phys.* **2016**, *93*, 115127.

(62) Malet, F.; Gori-Giorgi, P. Strong Correlation in Kohn-Sham Density Functional Theory. *Phys. Rev. Lett.* **2012**, *109*, 246402.

(63) Mendl, C. B.; Malet, F.; Gori-Giorgi, P. Wigner localization in quantum dots from Kohn-Sham density functional theory without symmetry breaking. *Phys. Rev. B: Condens. Matter Mater. Phys.* **2014**, *89*, 125106.

(64) Grabowski, I.; Lotrich, V. Accurate orbital-dependent correlation and exchange-correlation potentials from non-iterative ab initio dft calculations. *Mol. Phys.* **2005**, *103*, 2085−2092.

(65) Görling, A. Orbital- and state-dependent functionals in density-functional theory. *J. Chem. Phys.* **2005**, *123*, 062203.

(66) Stanton, J. F. et al. *ACES II*; Quantum Theory Project: Gainesville, FL, 2007.

(67) Colle, R.; Nesbet, R. K. Optimized effective potential in finite-basis-set treatment. *J. Phys. B: At., Mol. Opt. Phys.* **2001**, *34*, 2475.

(68) Dunning, T. H., Jr. Gaussian basis sets for use in correlated molecular calculations. I. The atoms boron through neon and hydrogen. *J. Chem. Phys.* **1989**, *90*, 1007−1023.

(69) Grabowski, I.; Hirata, S.; Ivanov, S.; Bartlett, R. J. Ab initio density functional theory: OEP-MBPT(2). A new orbital-dependent correlation functional. *J. Chem. Phys.* **2002**, *116*, 4415−4425.

(70) Widmark, P.-O.; Malmqvist, P.-Å.; Roos, B. O. Density matrix averaged atomic natural orbital (ANO) basis sets for correlated molecular wave functions. *Theoretica chimica acta* **1990**, *77*, 291−306.

(71) Peterson, K. A.; Dunning, T. H., Jr. Accurate correlation consistent basis sets for molecular core-valence correlation effects: The second row atoms Al-Ar, and the first row atoms B-Ne revisited. *J. Chem. Phys.* **2002**, *117*, 10548−10560.

(72) Seidl, M.; Di Marino, S.; Gerolin, A.; Nenna, L.; Giesbertz, K. J. H.; Gori-Giorgi, P. The strictly-correlated electron functional for spherically symmetric systems revisited. *arXiv:1702.05022 [cond-mat.str-el]* 2017.

(73) Wu, Q.; Yang, W. A direct optimization method for calculating density functionals and exchange-correlation potentials from electron densities. *J. Chem. Phys.* **2003**, *118*, 2498.

(74) Umrigar, C. J.; Gonze, X. Accurate exchange-correlation potentials and total-energy components for the helium isoelectronic series. *Phys. Rev. A: At., Mol., Opt. Phys.* **1994**, *50*, 3827.

(75) Filippi, C.; Umrigar, C. J.; Gonze, X. Separation of the exchange-correlation potential into exchange plus correlation: An optimized effective potential approach. *Phys. Rev. A: At., Mol., Opt. Phys.* **1996**, *54*, 4810.

(76) Kodera, M.; Miyasita, M.; Shimizu, H.; Higuchi, K.; Higuchi, M. Renormalized Møller-Plesset Correlation Energy Functional Used in the Optimized Effective Potential Method. *J. Phys. Soc. Jpn.* **2018**, *87*, 014302.

(77) Supporting Information.

(78) Schweigert, I. V.; Lotrich, V. F.; Bartlett, R. J. Ab initio correlation functionals from second-order perturbation theory. *J. Chem. Phys.* **2006**, *125*, 104108.

(79) Katriel, J.; Davidson, E. R. Asymptotic behavior of atomic and molecular wave functions. *Proc. Natl. Acad. Sci. U. S. A.* **1980**, *77*, 4403−4406.